Contribution from the Department of Chemistry,
University of Utah, Salt Lake City, Utah 84112

Crystal and Molecular Structure of the Tetrahydrofuran Adduct of (Vinylgallium)tetracarbonyliron, $[(THF)(C_2H_3)GaFe(CO)_4]_2$: Comparison with Isoelectronic Zinc and Germanium Dimers

JAN C. VANDERHOOFT, RICHARD D. ERNST,* F. WILLIAM CAGLE, JR.,* ROBERT J. NEUSTADT,
and TEDDY H. CYMBALUK

Received July 14, 1981

An X-ray diffraction study of $[(THF)(C_2H_3)GaFe(CO)_4]_2$ (THF = tetrahydrofuran) reveals a dimeric, planar, four-membered, metal–metal-bonded ring structure analogous to the isoelectronic $[(bpy)ZnFe(CO)_4]_2$ and $[(C_2H_5)_2GeFe(CO)_4]_2$ structures (bpy = 2,2′-bipyridine). Several distortions are observed in the structure that can be attributed to partial ionic character and the resultant bending of the axial carbonyl ligands over the metal ring. These distortions are intermediate in degree between those observed in the above-mentioned isoelectronic dimers and include a contraction of the M–Fe–M bond angle and a twisting of the idealized $Fe(CO)_4$ tetrahedra to opposite sides of the centrosymmetric dimers. The distortions arise in order to help maintain O_{ax}- - -O_{ax} nonbonded contacts at no less than ca. 3.04 Å. A number of comparisons have been made between the isoelectronic dimers. Other parameters of interest include Ga–Fe = 2.516 (3) Å, Ga–C = 2.069 (5) Å, Ga–O = 2.129 (4) Å, Fe–C(ax) = 1.775 (4) Å, Fe–C(eq) = 1.788 (3) Å, ∠Ga–Fe–Ga = 71.55 (4)°, ∠Fe–Ga–Fe = 108.45 (4)°, and $\angle C_{ax}$–Fe–C_{ax} = 156.85 (21)°. The structure has been refined (Mo K$\bar{\alpha}$ radiation) to a conventional R index (on F) of 0.036 for 2650 unique reflections having $I > 3\sigma(I)$. The space group is No. 2 (C_i^1—$P\bar{1}$), with a = 8.726 (3) Å, b = 8.871 (3) Å, c = 10.265 (5) Å, α = 99.59 (3)°, β = 103.91 (3)°, and γ = 116.14 (2)°.

Introduction

A number of studies dealing with the syntheses and structural natures of various associated, cyclic $[B_xMFe(CO)_4]_n$[1] and $[R_2M'Fe(CO)_4]_2$[2] (M = Zn, Cd, Hg; M′ = Ge, Sn, Pb; x = 1 or 2; n = 2 or 3; B = Lewis base) species have been reported. Our recent structural determination of the $[(bpy)ZnFe(CO)_4]_2$ dimer has finally revealed the key factors controlling the extent of association in these complexes, all of which contain an idealized cis-disubstituted iron coordination geometry.[1] These factors bring about the stabilization of ionic resonance hybrids that arise from a contribution of $Fe(CO)_4^{2-}$ species.[1,2] As this resonance contribution increases, the iron coordination geometry becomes more nearly bicapped tetrahedral than octahedral (see structures I and II). As can be seen, the ionic tetrahedral contribution brings about bending of the axial carbonyl ligands toward the ring center. For a small, dimeric ring, the bending tends to bring opposing axial oxygen atoms quite close, and it has been shown that the system's ability to relieve the resulting O_{ax}- - -O_{ax} interactions determines if a dimeric ring can be accommodated or whether a larger, trimeric ring is adopted,[1] as in the case of $[(bpy)CdFe(CO)_4]_3$.[1b]

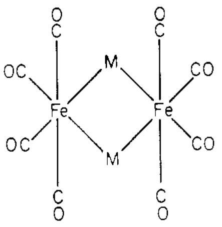

I

cis-disubstituted
octahedral
(covalent)

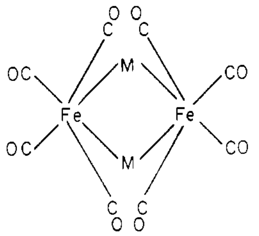

II

bicapped
tetrahedral
(ionic)

The particular distortions in question are nicely contrasted in the structures of the isoelectronic $[(C_2H_5)_2GeFe(CO)_4]_2$ and (the more ionic) $[(bpy)ZnFe(CO)_4]_2$ dimers.[1d,2a] As the previously described factors have led to the prediction that intermediate $(B)RGaFe(CO)_4$ complexes would also be dimeric,[1d] the structural parameters of such species are considered of interest because they allow precise examination of the extent of these molecular distortions as greater ionic character is induced in the complexes. Accordingly, such complexes were synthesized,[3] and we report herein the primary trends observed, which do correlate nicely with the given model.

Experimental Section

All operations involving organometallic carbonyls were carried out under an atmosphere of prepurified nitrogen in a Schlenk apparatus or in a glovebox. Nonaqueous solvents were thoroughly dried and deoxygenated in a manner appropriate to each and were distilled under nitrogen immediately prior to use. Disodium tetracarbonylferrate was prepared by a slight variation of our previously reported procedure.[3] This entails limiting the quantity of $Fe(CO)_5$ added to less than half the molar quantity of sodium amalgam and can be accomplished by decreasing the volume of $Fe(CO)_5$ to 8.0 mL in the previous method.

X-ray Diffraction Study of $[(THF)(C_2H_3)GaFe(CO)_4]_2$. $[(THF)(C_2H_5)GaFe(CO)_4]_2$ was prepared as previously reported.[3] Single crystals of the compound were grown by slow diffusion of pentane into a solution of the compound in THF at −20 °C. Many initial attempts to load the crystals were unsuccessful owing to their extreme thermal and air sensitivity. Nevertheless, two crystals were ultimately satisfactorily loaded. A combination of precession and Weissenberg photography was used in determining initial space group and unit cell data. These photographs indicated a triclinic space group which was assumed to be No. 2 (C_i^1—$P\bar{1}$).[4] At this point the second, higher quality crystal was loaded and transferred to a Syntex $P\bar{1}$ autodiffractometer equipped with a scintillation counter and pulse height analyzer. With use of standard software programs, the appropriate

---

(1) (a) Ernst, R. D.; Marks, T. J.; Ibers, J. A. *J. Am. Chem. Soc.* **1977,** *99,* 2090. (b) Ernst, R. D.; Marks, T. J.; Ibers, J. A. *Ibid.* **1977,** *99,* 2098. (c) Ernst, R. D.; Marks, T. J. *Inorg. Chem.* **1978,** *17,* 1477. (d) Neustadt, R. J.; Cymbaluk, T. H.; Ernst, R. D.; Cagle, F. W. *Ibid.* **1980,** *19,* 2375. (e) See also: Sosinsky, B. A.; Shelly, J.; Shong, R. *Ibid.* **1981,** *20,* 1370.

(2) (a) Zimmer, J. C.; Huber, Michel. *C. R. Hebd. Seances Acad. Sci., Ser. C* **1968,** *267,* 1685. (b) Gilmore, C. J.; Woodward, P. *J. Chem. Soc., Dalton Trans.* **1972,** 1387. (c) Harrison, P. G.; King, T. J.; Richards, J. A. *Ibid.* **1975,** 2097. (d) Hieber, W.; Breu, R. *Chem. Ber.* **1957,** *90,* 1270. (e) King, R. B.; Stone, F. G. A. *J. Am. Chem. Soc.* **1960,** *82,* 3833. (f) Kahn, O.; Bigorgne, M. *C. R. Hebd. Seances Acad. Sci., Ser. B* **1966,** *262,* 906. (g) Brooks, E. H.; Cross, R. J. *Organomet. Chem. Rev., Sect. A* **1970,** *6,* 227.

(3) Cymbaluk, T. H.; Ernst, R. D. *Inorg. Chem.* **1980,** *19,* 2381.

(4) "International Tables for X-ray Crystallography"; Kynoch Press: Birmingham, England, 1969; Vol. I, p 75.

0020-1669/82/1321-1876$01.25/0

Table I. Positional Parameters for the Atoms of $[(THF)(C_2H_3)GaFe(CO)_4]_2$

atom	*x*	*y*	*z*
Ga	0.050 34 (5)	0.022 41 (5)	0.152 22 (4)
Fe	0.270 09 (6)	0.132 92 (7)	0.025 40 (5)
C(1)	0.478 57 (53)	0.224 38 (63)	0.172 48 (47)
C(2)	0.354 51 (54)	0.182 34 (68)	−0.112 93 (48)
C(3)	0.228 67 (55)	0.310 24 (52)	0.070 17 (46)
C(4)	0.222 61 (55)	−0.089 00 (60)	−0.015 87 (45)
C(5)	−0.044 51 (74)	−0.305 56 (85)	0.265 57 (72)
C(6)	0.054 27 (78)	−0.366 57 (71)	0.361 69 (60)
C(7)	0.249 74 (85)	−0.232 60 (92)	0.406 44 (69)
C(8)	0.265 12 (69)	−0.147 41 (88)	0.298 27 (75)
C(9)	0.096 67 (66)	0.179 25 (57)	0.346 85 (50)
C(10)	0.259 44 (95)	0.282 60 (94)	0.430 85 (59)
O(1)	0.612 11 (43)	0.285 22 (58)	0.265 64 (37)
O(2)	0.404 59 (53)	0.207 71 (68)	−0.204 56 (44)
O(3)	0.208 73 (57)	0.428 82 (44)	0.100 89 (46)
O(4)	0.198 91 (55)	−0.230 64 (49)	−0.043 98 (42)
O(5)	0.088 23 (35)	−0.173 09 (35)	0.226 88 (30)

reduced cell was readily located. Accurate cell constants and their standard deviations were derived from a least-squares refinement of 15 centered reflections for which $30° < 2\theta < 45°$, by using the Mo $K\bar{\alpha}$ peak at 0.710 73 Å. The unit cell parameters are a = 8.726 (3) Å, b = 8.871 (3) Å, c = 10.265 (5) Å, α = 99.59 (3)°, β = 103.91 (3)°, γ = 116.14 (2)°, and V = 657.6 (4) Å^3 for Z = 2 monomeric units.

The crystal used for data collection displayed acceptable mosaicity for the θ–2θ scan technique. Mo $K\bar{\alpha}$ radiation was monochromatized by using the 002 face of mosaic graphite. Scans were taken from 1.3° below the Mo $K\alpha_1$ peak to 1.3° above the Mo $K\alpha_2$ peak at a rate of 1.5°/min. A collimator with a diameter of 1.0 mm was used as the crystal edges varied from 0.20 to 0.50 mm. Data were collected in a single shell of 2θ, 0–55°, with background time equal to half the total scan time. The intensities of five standard reflections were monitored for every 95 reflections and showed during data collection only relatively minor variations in intensity, and the intensity data were corrected for these variations.

All data were processed by using the X-RAY 70 program package.[5] A total of 3421 reflections were processed, yielding 3046 unique reflections, of which 2650 had intensities judged above background ($I > 3\sigma(I)$). These 2650 reflections were utilized in subsequent calculations. The function minimized was $\sum w(|F_o| - |F_c|)^2$, with empirical weights assigned in the latter stages by the method of Cruikshank.[6] The atomic scattering factors were taken from a recent tabulation, as were the anomalous dispersion terms for gallium and iron.[7]

The atomic coordinates of the gallium and iron atoms were each uniquely deduced from a Patterson map. All remaining nonhydrogen atoms were located on an ensuing difference Fourier map. After subsequent refinement, most hydrogen atom locations had become evident, so these 11 atoms were included in calculated positions. By this time it had become apparent that the molecules within the data crystal actually contained a vinyl group rather than the anticipated ethyl group bound to gallium. The origin of this change is unclear[8] but does not affect the structural details of interest. Anisotropic least-squares refinement led to convergence at R = 0.054 ($R = \sum||F_o| - |F_c||/\sum|F_o|$). The crystal faces were indexed as (001), (00$\bar{1}$), (011), (0$\bar{1}\bar{1}$), (01$\bar{1}$), (0$\bar{1}$1), (10$\bar{1}$), ($\bar{1}$01), (100), and ($\bar{1}$00) for the platelike crystal with approximate dimensions of 0.25 × 0.65 × 0.88 mm. After correction for absorption,[9] further refinement then led to convergence at R = 0.036 and R_w = 0.046 ($R_w = [\sum w(|F_o| - |F_c|)^2/\sum wF_o^2]^{1/2}$). A final difference Fourier revealed no peaks greater than 0.33 e/Å^3, with the standard deviation for the map being 0.07 e/Å^3. The final positional (Table I) and thermal (Table II, supplementary material) parameters obtained from the last cycle of least-squares refinement are presented along with their estimated standard deviations. Pertinent bond distances and angles are given in Table III. Root-mean-square amplitudes of vibration (Table IV) and a listing of the final values of $10F_o$ and $10F_c$ are available as supplementary material. Reflections for which the measured intensity was less than zero were assigned values of zero for F_o. Other than those mentioned later, the nonbonded contacts were normal.

Table III. Selected Bond Distances (Å) and Angles (Deg) for $[(THF)(C_2H_3)GaFe(CO)_4]_2$

Ga–Fe	2.510 (1)	Fe–C(3)	1.776 (5)	C(5)–O(5)	1.435 (7)
Ga–Fe′	2.521 (2)	Fe–C(4)	1.774 (5)	C(5)–C(6)	1.480 (11)
Ga–C(9)	2.069 (5)	C(1)–O(1)	1.141 (5)	C(6)–C(7)	1.479 (8)
Ga–O(5)	2.129 (4)	C(2)–O(2)	1.144 (7)	C(7)–C(8)	1.444 (12)
Fe–C(1)	1.794 (4)	C(3)–O(3)	1.146 (7)	C(9)–C(10)	1.266 (7)
Fe–C(2)	1.782 (5)	C(4)–O(4)	1.152 (7)	C(8)–O(5)	1.436 (7)

Ga–Fe–Ga′	71.55 (4)	Ga′–Fe–C(3)	84.14 (12)
Fe–Ga–Fe′	108.45 (4)	Ga′–Fe–C(4)	79.63 (14)
Fe–Ga–C(9)	120.43 (13)	Ga–C(9)–C(10)	119.0 (6)
Fe–Ga–O(5)	106.22 (10)	Ga–O(5)–C(5)	123.7 (4)
Fe′–Ga–C(9)	116.52 (16)	Ga–O(5)–C(8)	123.0 (3)
Fe′–Ga–O(5)	106.88 (6)	C(1)–Fe–C(2)	101.31 (21)
C(9)–Ga–O(5)	96.20 (18)	C(1)–Fe–C(3)	96.25 (23)
Fe–C(1)–O(1)	178.9 (5)	C(1)–Fe–C(4)	96.79 (23)
Fe–C(2)–O(2)	177.5 (4)	C(2)–Fe–C(3)	99.74 (27)
Fe–C(3)–O(3)	177.5 (4)	C(2)–Fe–C(4)	96.34 (25)
Fe–C(4)–O(4)	176.9 (5)	C(3)–Fe–C(4)	156.85 (21)
Ga–Fe–C(1)	98.30 (17)	C(5)–O(5)–C(8)	108.8 (5)
Ga–Fe–C(2)	160.37 (13)	O(5)–C(5)–C(6)	107.0 (5)
Ga–Fe–C(3)	77.30 (16)	O(5)–C(8)–C(7)	107.5 (5)
Ga–Fe–C(4)	81.95 (17)	C(5)–C(6)–C(7)	105.4 (6)
Ga′–Fe–C(1)	169.55 (17)	C(6)–C(7)–C(8)	105.8 (5)
Ga′–Fe–C(2)	88.88 (13)		

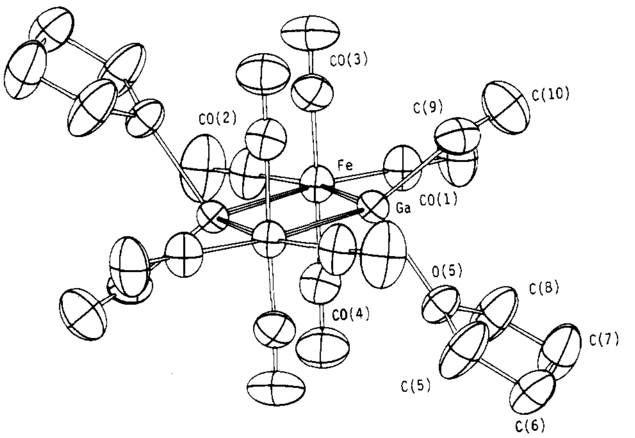

Figure 1. Perspective view for the centrosymmetric $[(THF)(C_2H_3)GaFe(CO)_4]_2$. The hydrogen atoms have been omitted for clarity.

Results

A perspective view of the centrosymmetric $[(THF)(C_2H_3)GaFe(CO)_4]_2$ molecule is presented in Figure 1 along with the atom numbering scheme. The hydrogen atoms have been omitted for clarity. Each has been assigned a number that first consists of the number of the carbon atom to which they are attached (1–10), followed by a sequential number (1–2) to distinguish between the hydrogen atoms on a given carbon atom. Due to the presence of a crystallographic inversion center, the four metal atoms in a given ring are rigorously

---

(5) Stewart, J. A.; Kundell, F. A.; Baldwin, J. C. "The X-ray System of Crystallographic Programs"; Computer Science Center, University of Maryland, College Park, MD, 1970.

(6) (a) Cruikshank, D. W. J. In "Crystallographic Computing"; Ahmed, F. R., Ed.; Munksgaard: Copenhagen, Denmark, 1970; pp 187–196. (b) The function used in this case was $w = (70.0 + |F_o| + 0.05|F_o^2| + 0.001|F_o|^3)^{-1}$.

(7) Cromer, D. T.; Waber, J. T. In "International Tables for X-ray Crystallography"; Kynoch Press: Birmingham, England, 1974; Vol. IV, Tables 2.2A and 2.3.1.

(8) (a) Only traces (<1%) of vinyl iodide were later found in the reagent grade ethyl iodide by gas chromatography. On standing for the prolonged periods, the compound is subject to some decomposition, so it is possible that some chemical interaction could be responsible (as observed in other metal carbonyls).[8b] (b) Shapley, J. R.; Tachikawa, M.; Churchill, M. R.; Lashewycz, R. A. *J. Organomet. Chem.* **1978**, *162*, C39.

(9) The absorption corrections were made by using a modified version of the Ibers program AGNOST.[1a]

planar. The equation of this plane and the distances by which the equatorial carbonyl ligands deviate from this plane are given in Table V (supplementary material).

The unique gallium atoms can be described as having a pseudotetrahedral coordination environment composed of two adjacent iron atoms, the attached carbon atom (C(9)) of the vinyl group, and the oxygen donor atom (O(5)) of the coordinated THF molecule. Essentially three of the six coordination angles about gallium are within a few degrees of tetrahedral (see Table III) while the other three are significantly distorted. Thus, the Fe–Ga–C(9) and Fe′–Ga–C(9) angles are 120.43 (13) and 116.52 (16)°, respectively, possibly indicative of an approach to ideal sp^2 hybridization on the gallium atom, with the THF oxygen atom presumably donating its electron pair to a gallium orbital of high p character. Indeed, the observed C(9)–Ga–O(5) angle of 96.20 (18)° is significantly reduced from the idealized tetrahedral value and comes close to the 90° value expected for gallium sp^2 hybridization. Similar observations have been made in other related base adducts and attributed to increased steric repulsions between more covalent bond pairs that are localized somewhat closer to the given metal atom.[10,11] In addition, a more covalent bond might prefer utilizing a lower energy orbital with higher s character (such as sp^2) while the weaker, essentially coordinate, bond(s) would involve an orbital of higher p character (Bent's rule). It may also be that steric crowding contributes to some of the observed unsymmetric gallium coordination geometry. For example, short intramolecular contacts are observed for O(5) (3.065 (6) Å from C(4)) and C(8) (3.310 (9) Å from C(4)) that probably prevent the THF molecule from making a closer approach to the gallium atom and thereby further decrease the importance of this bonding interaction.[12] This view is supported by a comparison of the present Ga–O bond distance of 2.129 (4) Å with the coordinate bond distances in related compounds.[13-16] It can further be pointed out that the Ga–C bond distance of 2.069 (5) Å also seems unusually long compared to other gallium alkyls (ca. 1.96 Å).[14,17-20] Once again nonbonded contacts (C(1)–H(3) = 2.89 Å, C(9)–O(5) = 3.124 (7) Å) may be responsible for the lengthening. Since the Zn–N bonds in $[(bpy)ZnFe(CO)_4]_2$ were also lengthened,[1d] it would appear reasonable to regard the $Fe(CO)_4$ groups as very large, sterically demanding ligands.

The two observed Ga–Fe bond distances differ slightly at 2.510 (1) and 2.521 (2) Å, averaging 2.516 (3) Å. This can be compared to the Zn–Fe distances in the isoelectronic $[(bpy)ZnFe(CO)_4]_2$, which differed even more at 2.532 (1) and 2.585 (1) Å.[1d] The much larger difference in that case may be due to hybridization influences on the zinc atom brought about by unsymmetric bipyridyl ligand packing, as discussed previously, while other subtle iron hybridizaton effects (vide infra) may be responsible in part for the differences in both cases. In contrast, the Ge–Fe bond distances in the more covalent, isoelectronic $[(C_2H_5)_2GeFe(CO)_4]_2$ compound were essentially equivalent at 2.492 (3) Å.[2a] This distance is shorter than the average Ga–Fe bond distance of 2.516 (3) Å by 0.024 Å, a difference nearly identical with the differences in single-bond metallic radii for gallium (1.245 Å) and germanium (1.223 Å).[21] However, the observed Zn–Fe bond distances of 2.532 (1) and 2.585 (1) Å seem particularly long considering that the single-bond metallic radius for zinc is 1.249 Å. In that structure a great deal of distortion and repulsive contact (O- - -O, Zn- - -Zn) was present and probably responsible for the apparent extension of these bonds. The fact that the two metal–metal bonds differ in length for both the gallium and the zinc structures will be discussed in more detail after a short examination of the nature of the distortions under consideration.

Due to the higher covalent character of $[(THF)(C_2H_3)GaFe(CO)_4]_2$ as compared to $[(bpy)ZnFe(CO)_4]_2$ (which is clearly observable in the infrared spectra),[1,3] there is less of a tendency for the axial carbonyl ligands to bend toward the ring center. Thus, the C_{ax}–Fe–C_{ax} angle of 156.85 (21)° for the present case is clearly more nearly linear than the corresponding angle of 150.05 (14)° observed in the zinc structure. The effect of this bending is that the iron coordination geometry approaches an extreme that may be described as having a tetrahedral $Fe(CO)_4{}^{2-}$ group capped by two metal ions (generally on faces, but in the case of $[(bpy)ZnFe(CO)_4]_2$ one of the caps actually occurs closer to a tetrahedral edge). However, in a dimeric structure, such bending tends to bring the opposite axial carbonyl ligands close together, as in II, and the resulting unfavorable O_{ax}- - -O_{ax} interactions bring about further geometric distortions in such a way as to relieve the O_{ax}- - -O_{ax} contacts (which here are 3.039 (6) Å). Thus, the Ga–Fe–Ga bond angle contracts to 71.55 (4) from 75.43 (12)° in $[(C_2H_5)_2GeFe(CO)_4]_2$[2a] (cf. 66.02 (2)° in $[(bpy)ZnFe(CO)_4]_2$).[1d] This has the effect of further separating the opposite iron atoms and hence the carbonyl ligands to which they are attached. By itself, however, this distortion is apparently unable to bring about sufficient relief of the intramolecular contacts. As a result, a second distortion is observed in which the two idealized $Fe(CO)_4$ tetrahedra twist to opposite sides (or gallium atoms) of the dimer, as in III. If taken far enough, this distortion can lead to a situation where one gallium atom caps a tetrahedral edge on a given $Fe(CO)_4$ while the other gallium atom would essentially cap a tetrahedral face. Ideally this would require a M–Fe–M angle of 54.74°. In the present case, this twisitng can readily be observed by the relative values of the Ga–Fe–C(1) and Ga′–Fe–C(2) angles, 98.30 (17) and 88.88 (13)°, respectively, corresponding to a twist of 4.71° for the equatorial carbonyls. The axial carbonyls, however, undergo an even greater twist of 9.76°. Some more detailed comparisons of these and other parameters for the isoelectronic

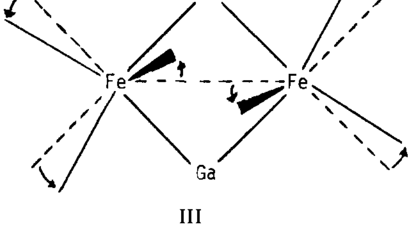

III

---

[10] Atwood, J. L.; Stucky, G. D. *J. Am. Chem. Soc.* **1967**, *89*, 5362.

[11] Widler, H.-J.; Schwarz, W.; Hausen, H.-D.; Weidlein, J. *Z. Anorg. Allg. Chem.* **1977**, *435*, 179.

[12] (a) These values may be affected to some extent by the obvious[12b,c] disorder occurring in the THF ligands. (b) Rietz, R. R.; Edelstein, N. M.; Ruben, H. W.; Templeton, D. H.; Zalkin, A. *Inorg. Chem.* **1978**, *17*, 658. (c) Cowley, A. H.; Cushner, M. C.; Davis, R. E.; Riley, P. E. *Ibid.* **1981**, *20*, 1179.

[13] Beamish, J. C.; Small, R. W. H.; Worrall, I. J. *Inorg. Chem.* **1979**, *18*, 220.

[14] Chong, K. S.; Rettig, S. J.; Storr, A.; Trotter, J. *Can. J. Chem.* **1979**, *57*, 586.

[15] Atwood, J. L.; Seale, S. K.; Roberts, D. H. *J. Organomet. Chem.* **1973**, *51*, 105.

[16] Beran, G.; Carty, A. J.; Patel, H. A.; Palenik, G. J. *J. Chem. Soc., Chem. Commun.* **1970**, 222.

[17] Breakell, K. R.; Rendle, D. F.; Storr, A.; Trotter, J. *J. Chem. Soc., Dalton Trans.* **1975**, 1584.

[18] Mertz, K.; Zettler, F.; Hausen, H. D.; Weidlein, J. *J. Organomet. Chem.* **1976**, *122*, 159.

[19] Rettig, S. J.; Storr, A.; Trotter, J. *Can. J. Chem.* **1975**, *53*, 58.

[20] (a) Indeed, one might have expected a shorter than usual Ga–C bond distance as a result of higher gallium s character as well as C→Ga pπ–pπ donation (cf. $(C_2H_3)_3B$),[20b] assuming the gallium p orbital has not been fully tied up by the THF ligand. (b) Holliday, A. K.; Reade, W.; Seddon, K. R.; Steer, I. A. *J. Organomet. Chem.* **1974**, *67*, 1.

[21] Pauling, L. "The Nature of the Chemical Bond", 3rd ed.; Cornell University Press: Ithaca, NY, 1960; Chapter 7.

Table VI. Selected Molecular Parameters, Distances (A) and Angles (Deg), for the Isoelectronic Dimers

parameter	metal		
	Ge	Ga	Zn
M-Fe	2.492 (3)	2.516 (3)	2.532 (1), 2.585 (1)
$\angle C_{ax}$-Fe-C_{ax}	162.0 (12)	156.85 (21)	150.05 (14)
$\angle C_{eq}$-Fe-C_{eq}	96.7 (15)	101.31 (21)	103.25 (16)
O_{ax}- - -O_{ax}	3.118 (26)	3.039 (6)	3.048 (4)
∠M-Fe-M	75.43 (12)	71.55 (4)	66.02 (2)
∠Fe-M-Fe	104.57 (14)	108.45 (4)	113.98 (2)
∠L-M-L	105.1 (11)	96.20 (18)	77.75 (8)
M- - -M	3.049 (5)	2.942 (2)	2.788 (1)
equatorial CO twist	0.53	4.71	11.01
axial CO twist	0.96	9.76	16.80
Fe-C_{ax}	1.756 (18)	1.775 (4)	1.758 (2)
Fe-C_{eq}	1.738 (21)	1.788 (3)	1.768 (3)

dimers will be made later (see Discussion).

The above distortions may partially explain the presence of two differing M-Fe bond lengths for the zinc and gallium structures. In each case the M-Fe bond that becomes lengthened is the one toward which the idealized $Fe(CO)_4$ tetrahedra have twisted. For example, because the (cis) Ga′-Fe-C(2) angle of 88.88 (13)° is smaller than the Ga-Fe-C(1) angle of 98.30 (17)°, it is the Ga′-Fe bond (or the equivalent Ga-Fe′ bond after inversion through the symmetry center) that is longer than the Ga-Fe bond. The origin of this effect may well be the hybridization of the iron atom.[22] As the $Fe(CO)_4$ tetrahedra twist to opposite sides, one gallium atom nearly resides on a tetrahedral face while the other tends to reside nearer a tetrahedral edge. By an inspection of diagram IV, it can be seen that as the distortion progresses, one M atom tends to occupy an essentially equatorial site of a trigonal bipyramid with the other M atom capping a trigonal face. Thus, the first Fe-M bond will approach sp^2 hybridization on iron while the second will utilize more d orbital character. Since the zinc structure undergoes more distortion, there will be a greater hybridization difference and hence a greater difference in the two M-Fe bonds as compared to the present case (ca. 0.05 vs. 0.01 Å). However, while this hybridization model accounts for the differing metal-metal bond distances, by itself it would also predict that the Fe-C_{ax} bonds would be shorter than the Fe-C_{eq} bonds when, in fact, the opposite is apparently observed for both the zinc (1.758 (2) vs. 1.768 (3) Å) and the present gallium (1.775 (4) vs. 1.788 (3) Å) structures. Of course, the "axial" carbonyls are really not axial in the compounds at hand, and the given model only deals with iron hybridization effects and not the further complications brought on by π-accepting ligands.[24] It should be noted, however, that even for $Fe(CO)_5$ the axial carbonyl ligands are closer to the iron atom than are the equatorial carbonyls (1.807 (3) vs. 1.827 (2) Å).[25]

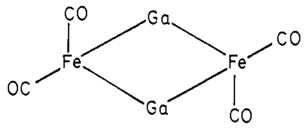

IV

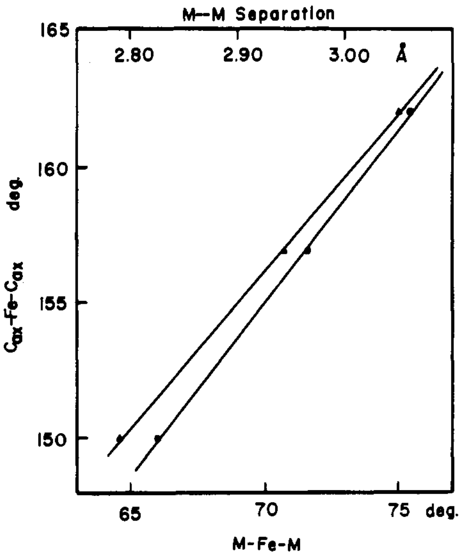

Figure 2. Dependence of ∠M-Fe-M and the M- - -M nonbonded contact on the extent of axial carbonyl bending. The upper line (triangles) corresponds to the upper absicissa, while the lower line (circles) corresponds to the lower abscissa.

Discussion

Now that the structural parameters pertaining to the $[(THF)(C_2H_3)GaFe(CO)_4]_2$ molecule have been considered, a more detailed comparison among the three isoelectronic dimer systems can be made. The pertinent bond distances and angles are summarized in Table VI. The key to all of the distortions is again the extent of ionic character in a given system, which determines how much of a role the bicapped tetrahedral resonance hybrids will play in the overall electronic makeup of the molecule. As can be seen in Table VI, on going from the more covalent germanium to the more ionic zinc complex, the carbonyl ligands are clearly deforming to a more nearly tetrahedral disposition, as evidenced by the decrease in the C_{ax}-Fe-C_{ax} angle and an increase in the C_{eq}-Fe-C_{eq} angle. As the C_{ax}-Fe-C_{ax} angle decreases, the O_{ax}- - -O_{ax} separation naturally should decrease. This appears to be the case in going from germanium to gallium, but then the separation levels off, being nearly equal at 3.04-3.05 Å for both the gallium and the zinc structures. To maintain a nearly equal oxygen atom separation, which clearly shows a repulsive nature,[26] two major distortions have taken place in the gallium and zinc compounds. First (Table VI), the M-Fe-M angle has contracted from 75.43 (14) to 66.02 (2)°, while the Fe-M-Fe angle has correspondingly increased from 104.57 (14) to 113.98 (2)° (this latter increase is accompanied by a corresponding decrease in the other L-M-L angles). While the contraction of the M-Fe-M angle does allow further separation of the axial carbonyl oxygen atoms, it also serves to bring the opposing M atoms closer together. This apparently reaches the point of severity for zinc, where the Zn- - -Zn contact of 2.788 (1) Å is essentially at a van der Waals separation.[23] Apparently, on the introduction of a larger, still somewhat ionic

---

(22) (a) Repulsive interactions between the gallium atoms and the nearer of the two equatorial carbonyls might also be considered. Even though these Ga-C distances are not in the range generally assigned to semibridging interactions,[22b,c] they are still much shorter than the sum of the appropriate van der Waals radii.[21,23] However, Ga-C(axial) contacts are even shorter and do not seem to have had any observable effect compared to $[(C_2H_5)_2GeFe(CO)_4]_2$. (b) Cotton, F. A. *Prog. Inorg. Chem.* **1976**, *21*, 1. (c) Dettlaf, G.; Weiss, E. *J. Organomet. Chem.* **1976**, *108*, 213.

(23) (a) Bondi, A. *J. Phys. Chem.* **1964**, *68*, 441. (b) Donohue, J. "The Structures of the Elements"; Interscience: New York, 1974.

(24) (a) Hoffmann, R.; Chen, M. M. L.; Elian, M.; Rossi, A. R.; Mingos, D. M. P. *Inorg. Chem.* **1974**, *13*, 2666. (b) Rossi, A. R.; Hoffmann, R. *Ibid.* **1975**, *14*, 365.

(25) Beagleu, B.; Schmidlung, D. G. *J. Mol. Struct.* **1974**, *22*, 466.

(26) (a) In view of the large van der Waals radius of carbon (1.7 Å)[20] one could also consider C_{ax}- - -C_{ax} separations, which actually are ca. 3.382 (6) Å. However, as we have already pointed out,[1d] the van der Waals radius of oxygen seems particularly large in directions perpendicular to multiple bond axes,[22a] and the C-O multiple bonds are somewhat localized on oxygen.[25b,c] In addition, the deviation from linearity of the Fe-C_{ax}-O_{ax} bong angles is in such a direction as to suggest more O_{ax}- - -O_{ax} interaction. (b) Fenske, R. F. *Prog. Inorg. Chem.* **1976**, *21*, 179. (c) Braterman, P. S. *Struct. Bonding (Berlin)* **1972**, *10*, 57.

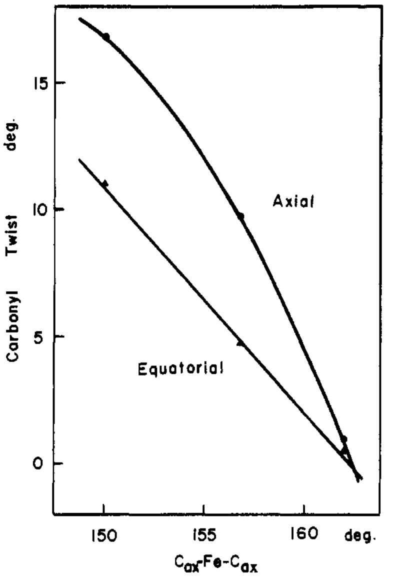

Figure 3. Dependence of the axial and equatorial twist deformations on the extent of axial carbonyl bending.

metal such as cadmium, a system is unable to alleviate both the O_{ax}- - -O_{ax} and the M- - -M contacts, so that a trimeric structure is observed. The fact that there is a good correlation between the axial carbonyl bending and either the M–Fe–M angle or the M- - -M nonbonded contact is clearly evident in Figure 2. Note that for each degree of axial carbonyl bending there results a decrease in the M–Fe–M angle of ca. 0.8°.

Besides the contraction of the M–Fe–M angle, a second distortion also takes place to help maintain the O_{ax}- - -O_{ax} separation at a nearly constant value. Both the axial and the equatorial carbonyls on a given iron atom twist to one side of the dimer, so that the corresponding carbonyls on the opposite iron atom twist to the opposite side. While the germanium structure can be seen to be nearly undistorted, substantial distortions are observed in the gallium and zinc structures (Table VI). The axial carbonyl twisting, defined by half of the difference between the angles made by the C_{ax}–Fe–C_{ax} plane with the Fe–M and the Fe–M′ vectors, increases to 16.80° for the zinc structure. The twisting of the equatorial carbonyls lags somewhat behind, reaching 11.01° for the zinc structure. This twisting is defined as one-half the difference between the (cis) C_{eq}–Fe–M and the (cis) C_{eq}–Fe–M′ angles. The extent of correlation between the C_{ax}–Fe–C_{ax} angle and the (axial or equatorial) carbonyl twisting for the various dimers may be observed in Figure 3. The correlation involving the equatorial carbonyls is linear within experimental error, with a 1.0° bend of the axial carbonyls bringing about a 1.1° twist of the equatorial carbonyls. A reasonable but nonlinear correlation also seems to be observed between the axial carbonyl twisting and the axial carbonyl bending. As should be expected, the two curves intersect essentially at a mutual carbonyl twisting angle of 0°. Thus, when ionic character is sufficient to cause the C_{ax}–Fe–C_{ax} angle to drop below ca. 162–163°, both twisting deformations are initiated concurrently. The origin of the nonlinearity of the axial carbonyl curve may be proposed to be the approach of each of the main-group metal atoms to a tetrahedral-edge-bridging configuration on one of the two $Fe(CO)_4$ groups to which they are attached as a results of the acute M–Fe–M angle.[27] If this edge-bridging configuration is substantially repulsive (perhaps even a local potential-energy maximum) compared to the tetrahedral-face alternative, it would naturally tend to suppress the extent of axial carbonyl twisting that occurred, resulting in the nonlinear behavior.

It has now become clear that the factors responsible for determining the extent of association in these metal–metal-bonded systems involve a combination of ionically induced axial carbonyl bending and a given system's ability to alleviate the resulting unfavorable O_{ax}- - -O_{ax} contacts by undergoing two principal deformations. That the systems at hand will undergo such great distortions without polymer or at least larger oligomer formation would indicate that the metal–metal bonds are extremely deformable. The result of this is that entropy seems to be the principal determining factor for the extent of association. It would appear, then, that if metal–metal-bonded polymers are to be prepared from these or similar systems, some other influences (e.g., imposition of a trans M–Fe–M coordination) will probably have to be found that can effectively counter the influence of entropy.

Acknowledgment. R.D.E. wishes to express his gratitude for partial support for this research through grants from the donors of the Petroleum Research Fund, administered by the American Chemical Society, from a Pennwalt Corp. Grant of Research Corp., and from the University of Utah Research Committee. We also thank Professor J. A. Ibers of Northwestern University for a copy of his X-ray programs.

Registry No. $[(THF)(C_2H_3)GaFe(CO)_4]_2$, 80441-09-4.

Supplementary Material Available: Listings of structure factor amplitudes, anisotropic thermal parameters (Table II), root-mean-square amplitudes of vibration (Table IV), least-squares plane data (Table V), and calculated hydrogen atom parameters (Table VII) (23 pages). Ordering information is given on any current masthead page.

---

[27] Some examples of edge-bonded metal compounds: (a) Simon, F. E.; Lauher, J. W. *Inorg. Chem.* **1980**, *19*, 2338. (b) Wilson, D. R.; Liu, J.-Z.; Ernst, R. D. *J. Am. Chem. Soc.*, in press.